Ber. nat.-med. Ver. Salzburg	Band 14	S. 183-208	Salzburg 2004

SECONDARY FLOWS IN BRONCHIAL BIFURCATION MODELS – INSPIRATION AND EXPIRATION

THOMAS HEISTRACHER[1,2] and WERNER HOFMANN[1]

Kurzfassung

Die Ablagerung von möglicherweise schädlichen Luftschwebeteilchen in der Lunge wird in hohem Maß von den Strömungsmustern der Atemluft beeinflusst, weshalb hier eine detaillierte Darstellung von Luftströmungen in dreidimensionalen Atemwegsmodellen vorgestellt wird. Aktuelle geometrische Modelle von Atemwegsverzweigungen, wie die ‚Physiologisch Realistische Bifurkation' (PRB), werden herangezogen, um mit der kommerziellen Strömungssimulationssoftware FIRE® Ein- und Ausatmungssituationen zu simulieren und zu diskutieren. Das Auftreten von primären (longitudionalen) und sekundären (transversalen) Strömungsanteilen hängt stark mit der Geometrie der Atemwegsverzweigung zusammen, im Speziellen mit den Details der Carina. Die Höhe der ortsabhängigen Sekundärströmungsanteile wird mit einem Intensitätsfaktor (SMIF) ausgedrückt und hier für gängige Atemsituationen untersucht. Beträchtliche Unterschiede zwischen Modellen mit klassischen (spitzen) und geglätteten (PRB) Verzweigungsstellen sind zu beobachten. Diese Ergebnisse können die bisherigen Interpretationen von Studien zur Aerosoldeposition in nicht so realitätsnahen Modellen von Atemwegsverzweigungen beeinflussen.

Schlüsselwörter: Atemwegmodelle, Strömungsmuster, Computergestützte Strömungsberechnungen, Sekundäre Strömungen

Abstract

Air flow patterns in the lungs strongly influence aerosol deposition characteristics of potentially harmful particulate matter. Thus an investigation of detailed characteristics of airflow in three-dimensional airway models is presented in this study. Current geometric models of airway bifurcations, such as the 'Physiologically Realistic Bifurcation' or PRB model, are utilized for the application of the commercial FIRE® CFD-package and discussed in detail for inspiratory and expiratory breathing conditions. Primary (longitudinal) and secondary (transversal)

flow components are found to be strongly related to bifurcation geometry, in particular to the shape of the carinal ridge. The magnitude of site-specific secondary flows is expressed by a 'secondary motion intensity factor' (SMIF) and discussed here for common breathing scenarios. Considerable differences in secondary flow intensity are encountered when comparing models with sharp (classical) and smooth (PRB) carinal ridge. The findings may affect the interpretation of deposition studies performed so far in less realistic bifurcation models.

Keywords: Airway models, Air flow patterns, Computational fluids dynamics, Secondary flows

Introduction

Deposition efficiencies in human airways are commonly used for risk assessment purposes. They are based on the assumption of homogenous distributions and thus may underestimate local dose effects in inhalation toxicology and aerosol therapy. Major determinants of localized particle deposition are the physiologic and geometric boundary conditions of the entraining flow. As non-invasive measurements are extremely difficult at this scale of detail, we chose to analyze air flow in bronchial airway bifurcation models, an idealized and a physiologically realistic bifurcation model.

In recent years, several authors have demonstrated the significance of the geometry of airway bifurcations on air flow and aerosol particle deposition (Asgharian and Anjilvel, 1994; Balásházy et al., 1996; Gradon and Orlicki, 1990; Heistracher et al., 1995; Martonen et al., 1995; Zhang et al., 2002). In particular, two bifurcation models were studied in more detail: (i) the standard bifurcation model with a sharp carinal ridge and three straight cylindrical parts (Balásházy et al., 1996), and (ii) the 'Physiologially Realistic Bifurcation' (PRB) model (Heistracher and Hofmann, 1995) with a defined curvature of the carinal ridge and a continuously shaped surface. These two models differ mainly in their central zone geometry, a region, which is of special interest for this paper.

Because of the large number of boundary conditions that occur in respiratory physiology, which are most often time dependent (Guan and Martonen, 2000), direct mathematical solution of the governing equations is not possible. Initiated by the availability of increased computer power, many investigators have attempted to study features of flow and deposition in selected geometries. But as demonstrated lately (Finlay et al., 1996; Oldham et al., 2000), special care has to be taken when interpreting the results of numerical calculations.

Analytical equations for inertial impaction and gravitational settling in circular bends have been derived by Balásházy et al. (1990). These authors conclude that analytical models cannot be used to characterize the differential distributions of deposition patters along the airways. Only for the calculation of total deposition do analytical models yield satisfactory results.

For health-related investigations, however, local deposition patterns are of paramount importance. Neither for the flow field nor for particle deposition in the vicinity of the rather complex carinae, can analytical solutions of the equations describing the acting mechanisms be derived. This is the reason for the recent increase in the application of numerical methods in fluid dynamics (Balásházy et al., 2003). For a deeper understanding of particle deposition in the lungs, a detailed knowledge of the particular airflow patterns occurring under different physiological conditions is crucial for interpreting and predicting health effects.
In this study, the development of primary (longitudinal) flows and particularly the development of secondary (transversal) flows for inspiratory and expiratory breathing conditions are investigated numerically for standard bifurcation units and for 'Physiologically Realistic Bifurcation' (PRB) units. Primary flows are moving in the direction of the prevailing air flow, whereas secondary flows represent the orthogonal components of that flow. Mass transport of air is driven by primary flows, whereas particle transport and, in consequence, particle deposition seems to be strongly influenced by secondary flows (cross streams). The computational scheme applied in this work is briefly discussed and geometric and micro-anatomical considerations are presented to clearly specify locations within bifurcation units. Air flow as the major determinant for deposition inhomogeneities is investigated for a variety of physiological breathing patterns, considering changes in minute volume, flow profile, and branching angle. As the airway bifurcation (bifurcation unit) is the structural element of the airway network, local and overall flow characteristics within the lungs are determined at this particular level of interest.

Geometric bifurcation model

Three dimensional airway models have been used by several authors (Asgharian and Anjilvel, 1994; Balásházy and Hofmann, 1995; Yung et al., 1990) and mathematical procedures have been published for the surface design of bifurcation units (Gradon and Orlicki, 1990; Heistracher and Hofmann, 1995; Zhao et al., 1992).
The 'narrow' bifurcation model was introduced by Balásházy and Hofmann, (1993) (Fig. 1). Structurally the 'narrow' model consists of three cylinders which are directly intersected forming a connecting zone with sharp edges to the parent and daughter branches. As will be discussed below, this model can be considered as a first approach to real bifurcation geometries. Although it exhibits major differences in flow and deposition patterns compared to more sophisticated models, it is the most suitable first advance in 3D modeling of bifurcating systems.
The 'wide' bifurcation model (Fig. 1, not used in this study) is an improvement of the 'narrow' model because of the reduced sharpness of the edges of the central zone, applying a 'constant azimuth angle condition' to generate the surface of one bifurcation (Balásházy, 1994). This model has been proposed by Balásházy and Hofmann (1993) as a reasonable compromise between the accuracy of the PRB model and the simplicity of the 'narrow' model (Hofmann et al., 2001).

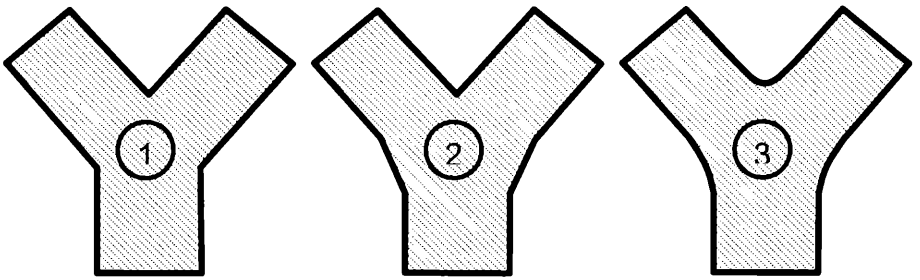

Figure 1 Schematic representation of three different bifurcation models: (1) narrow, (2) wide, and (3) 'Physiologically Realistic Bifurcation' (PRB).

The design of the geometric model used in this study is based on our recently developed mathematical description of a 'Physiologically Realistic Bifurcation' model (Heistracher and Hofmann, 1995), where the surface of a single arbitrarily shaped bifurcation is defined by a set of eleven parameters and two sigmoid functions (Fig. 1). Data on anatomical and micro-anatomical parameters have been incorporated into this airway bifurcation model (Horsfield et al., 1971; Hammersley and Olson, 1992; Martonen et al., 1994). Information on lengths and diameters is taken from the widely used Weibel (1963) and ICRP (1994) lung models. The whole geometry features a single, multiply curved surface and a carinal ridge without any sharp edge.

In contrast to the application of the commercially available CFD-package, the development of the three-dimensional mathematical bifurcation models was based on our own computer code written in the programming language C. There is no direct solution of the defining set of equations but when applying a two-parametric iteration-scheme (Heistracher and Hofmann, 1995), the surface of the bifuraction geometry can be calculated with strong convergence in the iteration scheme.

Figure 2 shows a top view of a bifurcation unit. Light gray shade indicates the parent branch, dark gray shades indicate the region of the daughter branches. In between these two regions is the so-called central zone located (no shades).

Secondary velocities are defined as flow components perpendicular to the prevailing main flow. Any flow velocity vector in an airway can be decomposed into an axial (longitudinal, primary) and a radial (transversal, secondary) component. This is clear for straight tubes (axis: parallel to axis of the cylinder; radial: perpendicular to axis), but for bifurcating airways this decomposition has to be based on clear definitions of the "axis" In this study, the axis in the central zone is given by center-points of the circles that establish the central zone surface (Heistracher and Hofmann, 1995),

which is the direction of the prevailing main flow in each of the daughter branches. The concept of decomposing the velocity vector is important for the understanding of the complex flow fields encountered in any kind of airway system, either technical or biological. Nevertheless it should be mentioned that secondary velocities do not represent a new physical quality of flow, but rather constitute a suitable physical parameter to describe the flow patterns in bifurcating geometries. In this study, the condition mentioned above is achieved by introducing cut-planes with clearly defined distances from the limiting planes of the central zone (planes 'P0r', 'D0r', and 'D0r'' in Fig. 2).

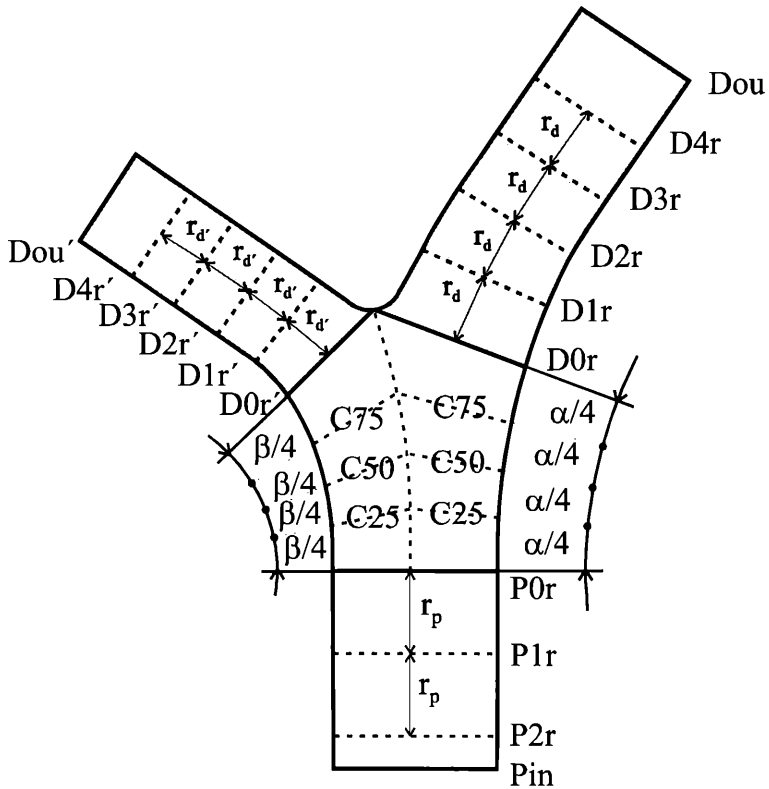

Figure 2 Notation for positions of cut-planes shown for a PRB model. For an explanation of the symbols, see related text.

These cut planes are perpendicular to the respective axes in the parent and daughter branches and, on a local scale, perpendicular to the prevailing main flow within the central zone. This concept facilitates both the production of physical airway models

for experimentation and mathematical and numerical analyses and comparisons of flow patterns, especially within the crucial central zone.
In this work, a three-character notation is used for locating cut-planes: The first character is either P for the parent branch, D for the daughter branches, or C for the central zone. For the parent and daughter branches, the second character is a number denoting the factor with which the adjacent radius (that is why 'r' is the third character in this notation) of the branch has to be multiplied to calculate the distance from the central zone limiting planes. For example, 'D1r' defines a plane in a distance of one daughter radius away from the central zone outlet 'D0r' (measured alongside the middle of the tube), and 'P2r' is a plane with a distance of two parent branch radii from the central zone inlet 'P0r'
For the central zone, the second and third digits represent the percentage of the branching angle that has to be covered when starting at 'P0r' in distal direction. For example, 'C25' is a central zone plane with a declination of 25% of the total respective branching angle relative to the central zone inlet 'P0r' With minor adaptations these definitions can easily be applied to any kind of experimental and theoretical bifurcation model, thus providing a feasible method for intercomparison of results from the open literature.

Computational Methods

For the calculation of the surface of the bifurcation models, a computer code written in the C programming language is applied to solve the governing equations that can be found in Heistracher and Hofmann (1995), using a two-parametric iteration procedure. Very detailed cross-sectional data in two dimensions result from this code. Sets of cross-sectional data are assembled in three dimensions to produce the surface of the bifurcation model, which is submitted to the preprocessor of a commercial software package. For the calculation of the air flow field in bifurcation units, the computational fluid dynamics (CFD) package FIRE® (AVL-List GmbH, Graz, Austria) has been applied. This is a general purpose CFD package based on a finite volume approach. Beside a very flexible adaptive mesh generation module (preprocessor), which is inevitable for smoothed surfaces in discrete meshes, it offers a variety of equation solvers to speed up convergence of the solution of the Navier-Stokes and continuity equations. By application of the FIRE® preprocessor, the surfaces of bifurcation models are "filled" with volume elements which resemble distorted cubes and constitute the numerical mesh for the calculations. It is a design goal to achieve a most homogenous distribution of numerical cells without introducing distorted cells. The PRB models discussed in this work consist of approximately 50,000 grid cells and the surfaces are mathematically defined according to Heistracher and Hofmann (1995).
For the comparison of radial (i.e., secondary) flow components, the 'Secondary Motion Intensity Factor' (SMIF) shall be used here (Heistracher, 1996; Hofmann et al., 2001). It is defined as the ratio of the local radial velocity maximum (e.g. at the

carinal ridge in plane 'D0r' or 'D0r'' of Fig. 2) and the average velocity in the corresponding branch. Thus high SMIF values indicate strong secondary motions.
The 'narrow' bifurcation was also used in this analysis to be able to verify the custom-made CFD code based on finite differences (Balásházy and Hofmann, 1993; Balásházy, 1994).

Flow results for inspiration

In this section the influence of the geometric boundary conditions on the flow field for a narrow and a PRB bifurcation for the inspiratory case is discussed. In general, flow conditions are more homogenous in the sense of less accentuated gradients in the PRB case, but the major differences occur close to the carinal ridge, revealing reverse flow conditions for the PRB model only.
To be able to judge the influence of the geometric boundary conditions on the flow field, identical breathing conditions of 10.2 m s^{-1} parabolic inspiratory flow were selected for this comparison. This velocity corresponds to heavy working conditions, resulting in a flow rate of 60 l min^{-1} in the trachea (ICRP, 1994). This relatively high value was selected to be able to discuss the secondary components of flow being more pronounced in this case. More moderate breathing conditions produce similar patterns, but they are not as illustrative as for higher flow rates, and will be discussed below. A branching angle of 35° is used here. The geometric details of both models are listed in Table 1.

Dimensions	'narrow' model	PRB model
Length of parent branch [m]	7.6E-3	7.6E-3
Length of daughter branches [m]	12.7E-3	12.7E-3
Diameter of parent branch [m]	5.6E-3	5.6E-3
Diameter of daughter branch A [m]	4.5E-3	4.5E-3
Diameter of daughter branch B [m]	4.5E-3	4.5E-3
Branching angle for branch A [°]	35/60	35/60
Branching angle for branch B [°]	35/60	35/60
Carinal ridge curvature radius [m]	-	0.9E-3
Curvature radius of branch A [m]	-	11.25E-3
Curvature radius of branch B [m]	-	11.25E-3

Table 1 Geometric data of the two symmetric bifurcation models discussed in this work.

We will now start a 'journey' through the two different bifurcation units, i.e. the 'narrow' and the PRB model for the case of 'parabolic' (that is the pattern of the flow profile at the inlets) inhalation with a 60 l min^{-1} flow rate. First, the axial flow components in the plane of bifurcation will be discussed, which are normal to the plane of the bifurcation, and at the cut-plane locations displayed in Fig. 2. Then the secondary velocities, i.e., the radial components of the flow (Isabey and Chang, 1982) will be compared for the narrow bifurcation and the PRB model at this series of cut-plane locations.

The absolute maxima of axial flow velocity for the inspiratory cases discussed do not differ significantly (up to 9.2% in plane 'C25', see Fig. 3), but there are some differences in the structure of the axial flow fields. There is an almost linear decrease up to position 'D0r' for the 'narrow' model, whereas the PRB reveals slightly higher values within the parent branch. It is noteworthy that downstream from here the velocity maxima for the daughter branch rise ('D1r') before they start to (rather monotonically) decrease to the value at the daughter branch outlets. This is a first indication of the complicated flow situation close to the carina in downstream direction and the back propagation effects of flow conditions in the central zone to the parent branch.

Parabolic flow characteristics predominate the axial flow fields, except for the 'P0r' location for the 'narrow' model, where increased gradients of axial velocity can be found in four places (Heistracher, 1996). As will be discussed later in this text, this is related to the pronounced widening of the 'narrow' model at the onset of the central zone, which causes strong secondary motions at this specific location. In contrast, the PRB model presents this effect in a much diminished manner. It can be stated that the flow profiles for positions 'P0r' deviate from the parabolic form mainly in the vicinity of the walls, where steeper velocity gradients are found.

The axial flow characteristics are quite similar for the 'narrow' and the PRB model. In general, (see the following discussion below), the PRB model reveals smoother velocity gradients compared to the 'narrow' model.

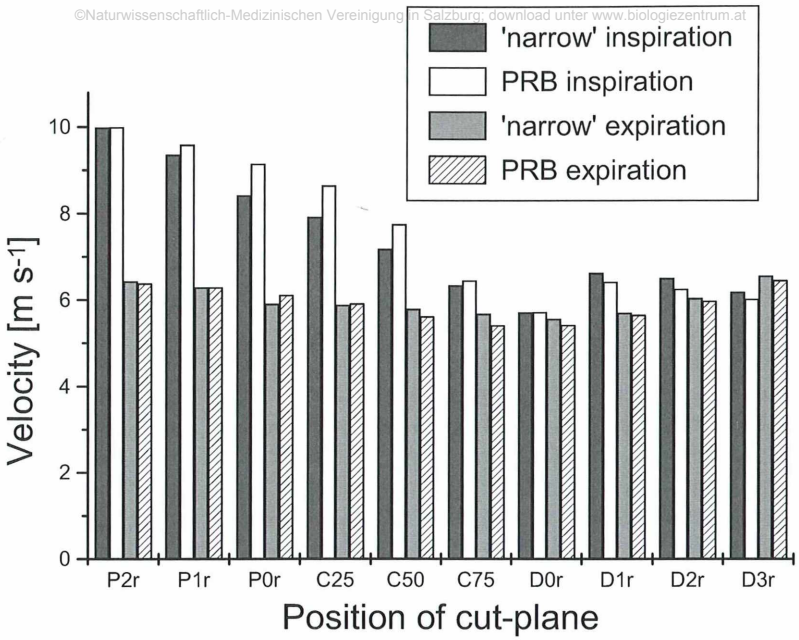

Figure 3 Comparison of the local maxima of axial velocity in 11 cut-planes for inhalation and exhalation, both for the 'narrow' and the PRB model.

Axial flow isoline representations for the 'D1r' location and downstream to the 'D4r' location for both the 'narrow' and the PRB model show (Heistracher, 1996) that except for the carinal position, the axial flows within the daughter branches do not differ appreciably from each other. In addition, there is at most a difference of 4% in the amount of the local velocity maximum.

Distinct 'dead water zones' immediately after the onset of the central zone can be found, whereas the extension of this low velocity region for the PRB model is very small and almost orientated parallel to the surface of the central zone. This is certainly related to the sharp edge of the 'narrow' bifurcation model at the onset of the central zone. Air molecules belonging to the boundary layer within the parent branch cannot be accelerated sufficiently to fill the space downstream of this central zone wedge immediately. Thus inertia is the reason for the marked 'dead water zone' in the 'narrow' model. Apparently the air molecules in the PRB model have sufficiently time to remain in the boundary layer (and close to it), and that is why there is no such accentuated low velocity region.

A second finding is the reduced gradient of axial velocity when approaching the carinal ridge from the parent branch. Due to the flattened area around the carinal

ridge in the PRB model, a larger high pressure region can be established, which reduces primary flow speed when approaching the carinal position for inspiration. The 'narrow' model, however, has a locally restricted high pressure region, and thus velocity gradients approaching the carinal ridge in this model are much more pronounced. This may have a major impact on particle deposition, as the residence time of air in the PRB model is increased in the vicinity of the carinal ridge compared to the 'narrow' model.

The asymmetry of the flow downstream the carinal location in each daughter branch is very pronounced for this high inspiratory flow rate. A slight local velocity maximum is present at a location about 0.5 daughter radii downstream of the carinal location. This can be explained by the merging of the secondary flow vortices at this site, which is displayed in the series of secondary velocity figures to be discussed below in this text.

The vector representations of the figures presented in this work are taken at 'half density' compared to the calculated numerical flow results. This is done to clearly demonstrate the main features of flow. In the vector plots of Figs 4 to 7, the scaling is different for each panel to achieve the best representation of the secondary velocity patterns. When comparing absolute values, the local maximum of the velocity listed for each panel has to be used. This is the radial velocity represented by the longest vector in each panel. The SMIF value is the fraction of maximum velocity and average branch velocity (as indicated by ranges).

Figure 8 gives a comparison of this SMIF factor for different locations for a 'narrow' and a PRB model in the case of inspiration. It should be noted that till now there are no data available for flow quantities within the central zone of bifurcating tubes, as the exact definition of cut-planes is quite difficult for smoothly curved geometries. As discussed earlier, the PRB model allows an elegant way to define the location of these plains. In general, the PRB model exhibits reduced SMIF values compared to the 'narrow' model for inhalation, except for the 'C25', 'C50', and 'D0r' locations, where it slightly exceeds the values for the 'narrow' model by 8.0%, 3.7%, and 5.1%, respectively.

Immediately after entering the parent branch, a slight tendency for air to spread to the outer sides of the parent branch can be found. Although the magnitudes of the secondary components are quite low (SMIF values are 0.043 and 0.029, respectively) this may be related to the upstream influence of the pressure field in the central zone. At position 'P1r', a slightly more intensive onset of outbound flow can be found, but the SMIF values are low for both cases (0.031 and 0.024, respectively). A tendency to the onset of rotational flow can be found at this location too.

Directly at the upstream end of the central zone both models reveal similar characteristics for the secondary velocity components, but the 'narrow' model in a more accentuated manner, i.e. the SMIF values are 3.6 times higher in the 'narrow' model as compared to the PRB model. Clearly a pronounced flow component in the directions of the daughter branches can be found, revealing once more that the upstream influence of the flow in the bifurcating region cannot be neglected. Flow

components directed away from the upper and lower walls of the parent branch can be observed, which indicate that both the narrowing of the height in the flow channel and the splitting of the flow into two directions causes the onset of strong secondary vortices.

The most striking differences between the 'narrow' and the PRB model do occur in the central zone. The double vortex pattern at the downstream beginning of the daughter branches has been published by several authors (Schroter and Sudlow, 1969; Isabey and Chang, 1982; Kinsara et al., 1993; Hammersley and Olson, 1992). However, no detailed flow information is available for the flow situation in the middle of the central zone, where the onset of the double vortex takes place, except for three publications of one research group (Zhao et al., 1992; Zhao and Lieber, 1994a, 1994b).

Caused by the very strong outbound flow at location 'P0r', the 'narrow' model shows a more complicated flow situation at cut-plane 'C25' (Fig. 4). Here a region with vanishing secondary velocity components can be found. This is the place where the 'dead water zone' discussed earlier in this section finds its largest extension. At this precise location, the outbound flow dominates the zone close to the outer wall, whereas inbound (secondary) flow governs the more central region in this cut-plane. The situation in the PRB model is quite different, because only inbound velocity components can be found here.

This condition continues to the 'C50' location, although inbound secondary flow begins to dominate in the 'narrow' model, whereas in the PRB the field is hardly changed compared to the more upstream cut-plane. The SMIF values amount to 0.403 and 0.366, respectively.

At the 'C75' cut-plane the SMIF values differ by about 65% (0.526 and 0.319), but the (secondary) flow patterns have become quite similar now. So the major finding for the flow situation in the central zone for inspiration is that there is a quite complicated flow situation in both cases, with the 'narrow' model being the earliest in establishing the double vortex pattern in downstream direction thus supporting the hypothesis of back propagation of flow conditions.

The most important site of investigation is the vicinity of the carinal ridge as this is the preferential place for particle deposition for inspiratory breathing conditions for particles larger than 0.5 μm and for particles of less than 0.5 μm of aerodynamic diameter (Balásházy and Hofmann, 1993; Balásházy et al., 2003).

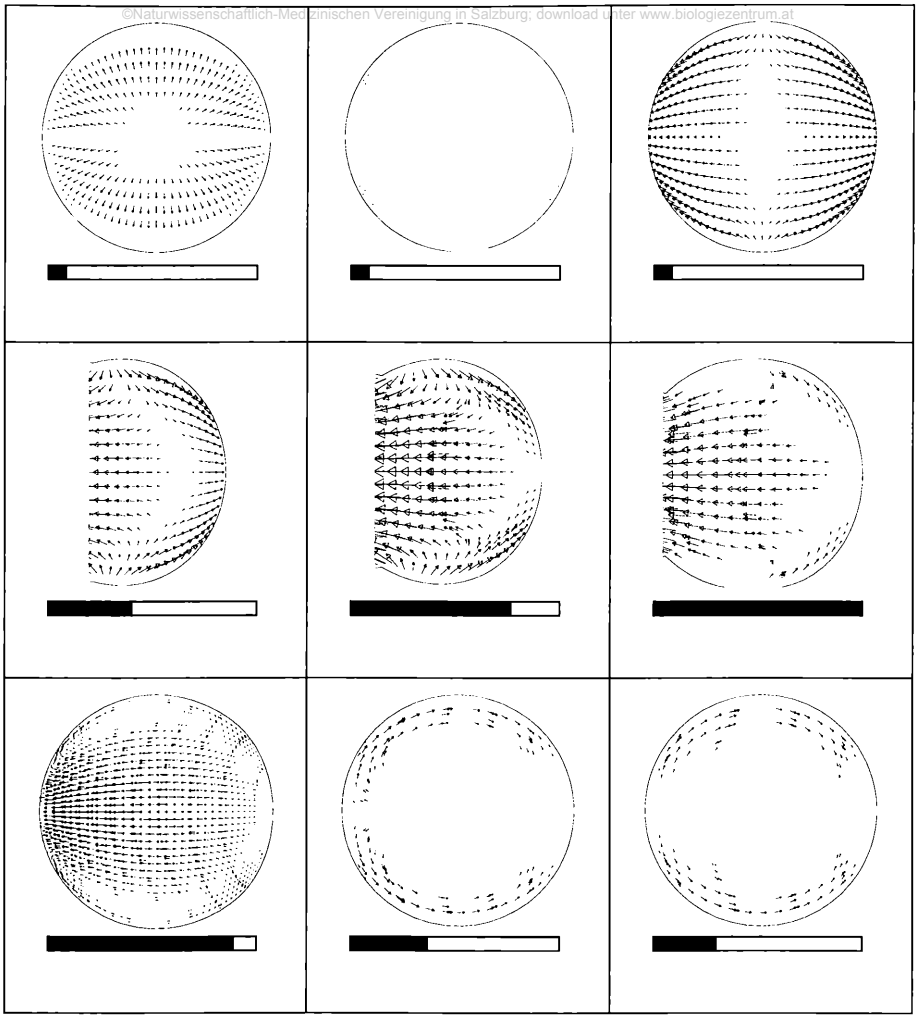

Figure 4 Development of secondary flows for inspiration in a 'narrow' bifurcation model. Secondary flow patterns and corresponding SMIF values (bar indicator from 0 to 100% of 0.526 ($SMIF_{max}$)) for a series of cut-planes perpendicular to the prevailing flow direction. Panels from top left to bottom right represent positions 'P2r', 'P1r', 'P0r', 'C25', 'C50', 'C75', 'D0r', 'D1r', and 'D2r', respectively.

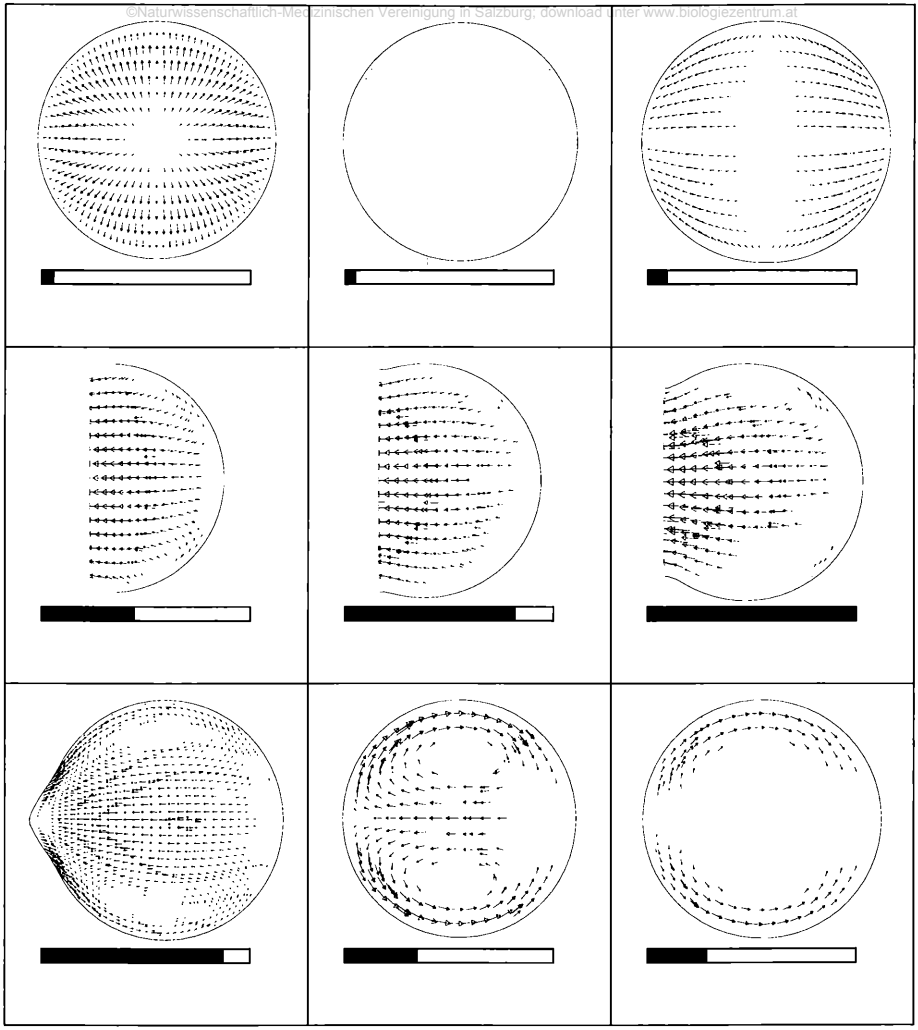

Figure 5 Development of secondary flows for inspiration in a PRB model. Secondary flow patterns and corresponding SMIF values (bar indicator from 0 to 100% of 0.513 ($SMIF_{max}$)) for a series of cut-planes perpendicular to the prevailing flow direction. Panels from top left to bottom right represent positions 'P2r', 'P1r', 'P0r', 'C25', 'C50', 'C75', 'D0r', 'D1r', and 'D2r', respectively.

The predominant direction of secondary flow in a 'narrow' bifurcation is towards the dividing spur of the geometry (carinal ridge; see Position 'D0r' in Fig. 4). This means that particles, which practically follow the streamlines of the air, i.e. with aerodynamic diameters around 0.5 µm (Ultman, 1985), will predominately deposit at or close to the carinal ridge. For the PRB model the situation is completely different as there is a flow component directed *away* from the site of the carinal ridge. As could be expected, the main mass transport in the parent branch is centered around the axis of the parent branch, especially in the case of parabolic inspiratory conditions, and so the flow can only be directed onto the site of the carinal ridge. But vectors are pointing toward the position of the axis of the daughter branch, which is in the center of the cross-section shown. The width of this region is about 10% of the daughter diameter.

The typical twofold vortex pattern downstream of the central zone has been described by experimental (Schroter and Sudlow, 1969; Isabey and Chang, 1982; Pedley, 1977) and theoretical (Kinsara et al., 1993; Heistracher and Hofmann, 1994) studies. Compared to the carinal position, the SMIF factors are quite reduced here, the patterns are rather similar for the 'narrow' and the PRB model, but the latter reveals smoother forms compared to the former. The reason may be that the flow velocity gradient (primary and secondary flow) found in PRB models is generally less pronounced compared to the 'narrow' and 'wide' models. So the less distorted velocity field in the central zone has its influence on the flow pattern in the daughter branches.

The situation two daughter diameters downstream of the carinal ridge reveals that here the secondary velocity patterns are very similar to each other, the twofold vortex pattern is less pronounced one daughter diameter upstream, and the SMIF factors (0.077 for the 'narrow' and 0.080 for the PRB model) are practically the same for both models. Figure 8 compares SMIF values in 'narrow' and PRB models for inspiration conditions. Except for plane 'P0r', SMIF values do not differ significantly. At location 'P0r', the 'narrow' model exhibits a four times higher SMIF value compared to the PRB model, which is related to the sharp edge at the central zone inlet.

Flow results for expiration

As for the inspiratory case, the expiratory flow conditions will be discussed by comparing a 'narrow' bifurcation and a PRB model. The same physiological breathing conditions are applied, finding similar flow patterns in the parent and the daughter branches for both models. However, the central zone reveals complicated flow conditions, which are different for both models.

To facilitate comparison, the same minute volume and the same type of inlet profile was selected for the two cases of the 'narrow' and the PRB model. A flow rate of $60\,l\,min^{-1}$ corresponds to a $7.9\,m\,s^{-1}$ maximal inlet velocity when applying a parabolic profile. This situation again represents heavy working conditions (ICRP,

1994). The outlet for expiration is the proximal parent branch end. The branching angle used here is 35° (geometric details of the models are listed in Table 1).
In contrast to the case of inspiration, axial velocity maxima do not differ significantly when comparing 'narrow' and PRB models for expiration (Fig. 3). As in the case of inspiration, the 'narrow' model reveals an extreme flow velocity gradient close to the proximal end of the central zone (Heistracher, 1996). This may result in a reduced probability of deposition of particles in the parent branch, because a kind of 'jet stream' is washing out midsize and larger particles from the vicinity of the wall of the central zone and thereby away from the surface of the parent branch.
The axial flow situation in the parent branch is quite the same for the 'narrow' and the PRB model, except for the fact that the twofold maxima of axial flow seem to remain longer in downstream direction in the 'narrow' model as compared to the PRB model (Heistracher, 1996). Once again, this finding shows a calmer flow situation in the PRB model.
The pressure field for expiration is quite similar to the pressure field for inspiration. As mentioned above, the measurement of the pressure distribution is extremely difficult as the traverse pressure difference has the same order of magnitude compared to the downstream pressure drop.
As for the case of inhalation we will now follow the air flow, thereby starting at the distal daughter branch ends approaching the carinal position and proceeding to the exit, which is here the parent branch.
Within the daughter branches practically the same flow situation prevails as in the inspiratory case at the inlet: a weak tendency of the secondary flow to the walls can be found at the daughter branch inlets with SMIF values of 2.9% for the 'narrow' and 2.6% for the PRB model (Figs 6 and 7). This once again may be related to the influence of the boundary layer, which establishes itself when viscosity is not neglected. The situation is the same 1.5 daughter branch diameters from the carinal ridge, but with SMIF values reduced by about 25% compared to the more distal location. At 1 and 0.5 daughter diameters from the carinal ridge, the radial velocities are practically the same for both models, and the SMIF values differ by less than 10%.
Figure 6 shows the secondary flow components at the distal end of the central zone for the 'narrow' model (the carinal position). Here an outflow almost parallel to the plane of the bifurcation can be found, whereas the PRB model (Fig. 7) exhibits a more 'rotational' picture: there is a location with vanishing secondary velocity in a distance of 0.3 daughter radii from the carinal ridge. This indicates that the evolution of the characteristic vortex patterns found for exhalation (Schroter and Sudlow, 1969) starts earlier in the PRB than in the 'narrow' model.
As for the case of inhalation, the secondary velocity components of the 'narrow' model close to the carina are reversed compared to the PRB model. Again this finding may have important implications for risk assessment studies. From the figures presented in this work for inspiration and expiration, however, it could be

concluded that the net effect on deposition probability can possibly be neglected as the separate effects of inspiration and expiration work in opposite directions.

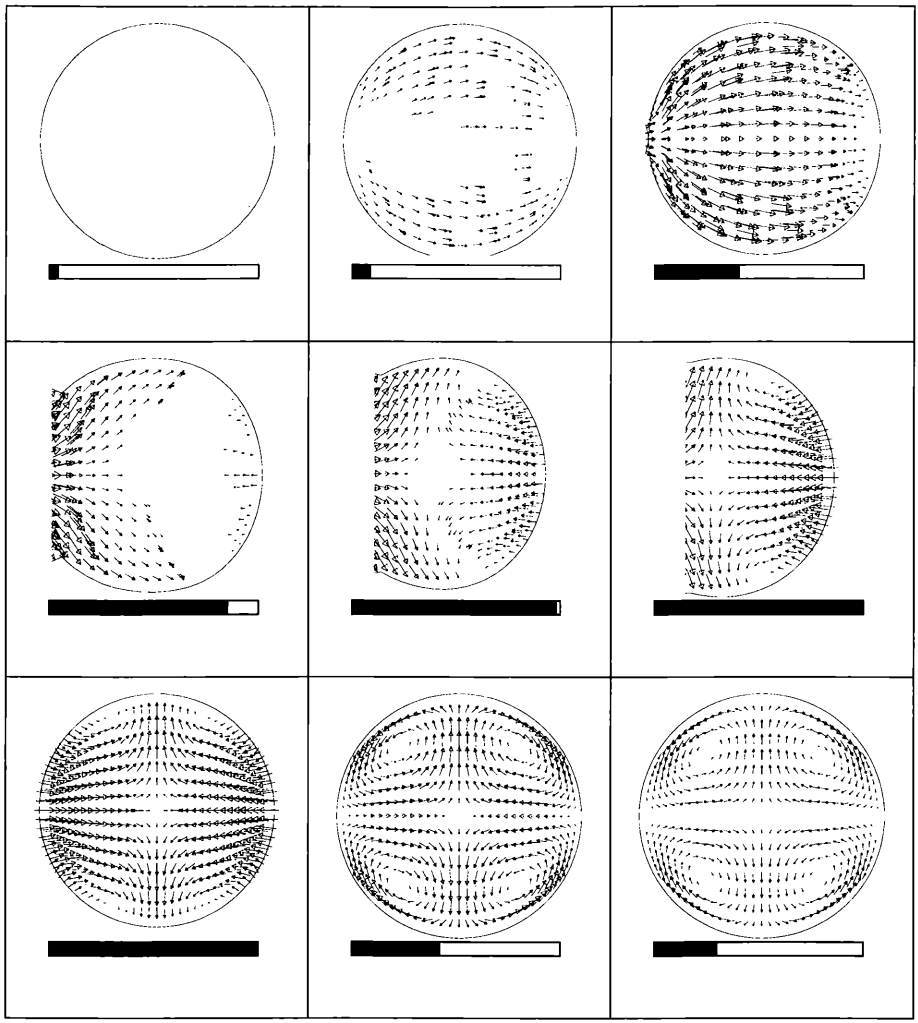

Figure 6 Development of secondary flows for expiration in a 'narrow' model. Secondary flow patterns and corresponding SMIF values (bar indicator from 0 to 100% of 1.905 ($SMIF_{max}$)) for a series of cut-planes perpendicular to the prevailing flow direction. Panels from top left to bottom right represent positions 'D2r', 'D1r', 'D0r', 'C75', 'C50', 'C25', 'P0r', 'P1r', and 'P2r', respectively.

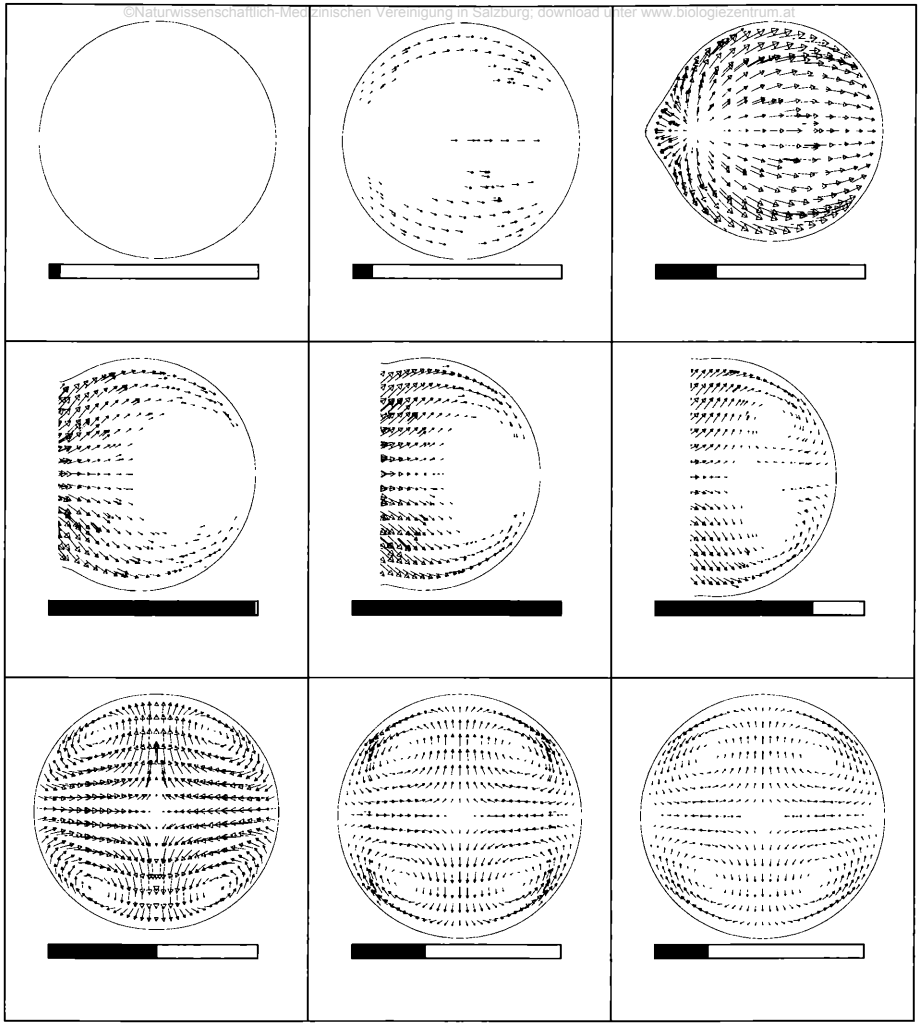

Figure 7 Development of secondary flows for expiration in a PRB model. Secondary flow patterns and corresponding SMIF values (bar indicator from 0 to 100% of 1.559 ($SMIF_{max}$)) for a series of cut-planes perpendicular to the prevailing flow direction. Panels from top left to bottom right represent positions 'D2r', 'D1r', 'D0r', 'C75', 'C50', 'C25', 'P0r', 'P1r', and 'P2r', respectively.

Although the SMIF factors for positions 'C75' are practically the same for both models (SMIF = 0.319 and 0.300), the secondary flow patterns differ: in the 'narrow' model there is a 'band' of vanishing radial flow in the middle of the cross section and a marked inbound flow contribution from the outer side of the central zone, which is shown in Fig. 6. The PRB model does not exhibit the marked radial component (Fig. 7), which may be related to the lack of a sharp edge connecting the daughter branches with the central zone.

In the middle of the central zone (Figs 6 and 7), the PRB model clearly shows a double vortex pattern, whereas the 'narrow' model again exhibits major inbound components. This situation is even more pronounced at the 'C25' locations, showing once again that the velocity gradients in the 'narrow' model are much higher than in the PRB model. In the PRB model, rotational flow clearly is established, whereas in the 'narrow' model the inbound components predominate due to the 'jet stream' effect of the sharp edge connecting the central zone with the parent branch. This again will have influence on aerosol particle deposition.

At the proximal end of the central zone the flow situation again becomes more similar for both models examined, but the SMIF factor for the 'narrow' model is 2.4 times higher than for the PRB model. From Figs 6 and 7 it can be seen that at the proximal end of the central zone (and only there) the site of the maximum of axial velocity coincides with the site of maximal radial (secondary) velocity. Considering aerosol particle deposition, the 'narrow' model once again shows major differences to the more physiological PRB model, because it seems to overemphasize the effects of secondary flow on deposition.

The 'P1r' location of the 'narrow' model is more similar to the 'P0r' location of the PRB model (except for steeper gradients and elevated SMIF values in the 'narrow' model) than to the same ('P1r') location, that is why the selection of cut-planes could be questioned.

At the 'P2r' location, the patterns of radial flow components do not differ markedly (Figs 6 and 7), but SMIF values are 11.3% for the 'narrow' model and 7.8% for the PRB model.

Figure 9 gives a comparison of the magnitudes of the SMIF factors for exhalation for the geometries examined in this chapter. As mentioned above, this factor is an overall estimate of the strength of the radial velocities and thus can be considered to be a measure of quality of the geometric model used, as (biological) evolution in general tends to optimize energy consumption (Tsuda et al., 1990), which should be valid for lungs too.

Approaching the central zone from the daughter branch outlets the SMIF values are practically the same for the 'narrow' and the PRB model, whereas the situation in the central zone dramatically differs, as discussed above. The SMIF value at the downstream end of the daughter branch is more than twice as high for the 'narrow' model compared to the PRB model (0.374 compared to 0.158, respectively). Even at the exit point, SMIF is raised by 45% for the 'narrow' model.

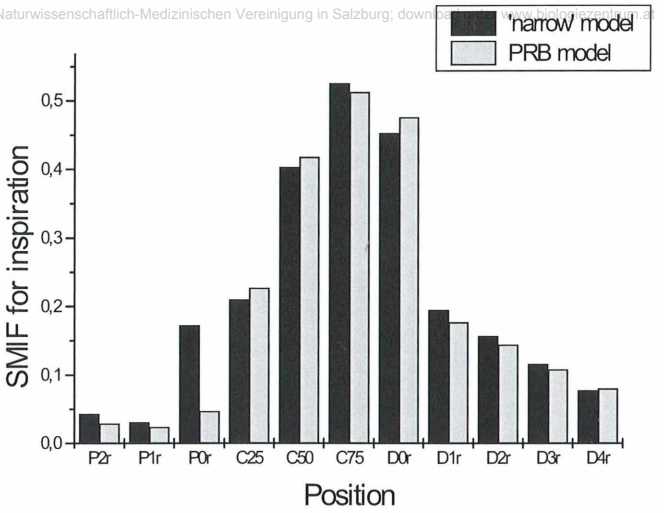

Figure 8 Comparison of SMIF values for inspiration for the 'narrow' and the PRB model at all cut-plane locations examined.

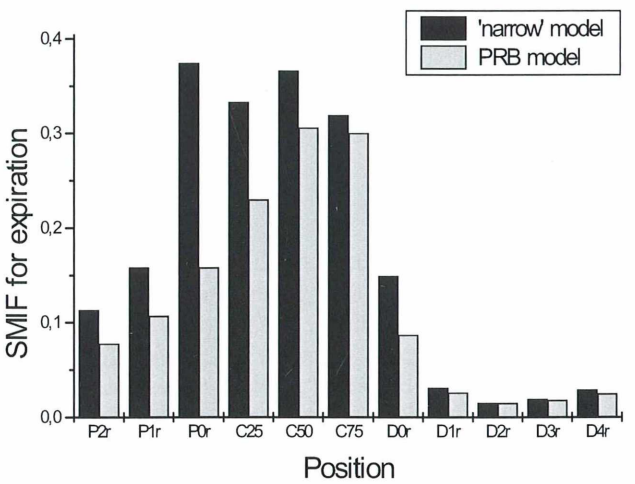

Figure 9 Comparison of SMIF values for expiration for the 'narrow' and the PRB model at all cut-plane locations examined.

Another geometric boundary condition is worth to be examined with respect to flow processes. Branching angles have paramount influence on the developing lengths of flow, as recently shown by Guan and Martonen (2000) in their bent tube studies. Thus the axial velocity components in the plane of the bifurcation and orthogonal to this direction are compared for the 'narrow' and the PRB model in this study for branching angles of 35° and 60° In addition, the influence of the branching angle on secondary motions, SMIF values for a tracheal flow rate of 120 l min^{-1} shall be discussed briefly.

For inspiration, there is no marked difference when entering the parent branch (Fig. 10, locations 'Pin' to 'P1r'). Downstream of location 'P0r', however, the 35° branching has increasingly higher SMIF values (up to location 'D0r') compared to the higher branching angle. From then on the 60° branching reveals higher SMIF values. This is again an indication that the upstream effects of primary and secondary flow cannot be neglected. Although the outer curvature of the central zone in the models compared is identical, a kind of rectification of flow seems to be enforced by the geometry with the smaller branching angle, therefore leading to elevated SMIF values in the central zone.

As would be expected, the secondary velocities downstream of the central zone are higher for the higher branching angle (Fig. 10), reflecting the continued radial acceleration of air up to the straight section of the daughter branches.

The development of SMIF values for expiration is displayed in Fig. 11. When starting at the daughter branch ends (right side of Fig. 11) the situation from locations 'Dou' to 'D3r' is quite similar. The 60° branching, however, exhibits a marked increase in SMIF from the 'D2r' position to the 'D0r' position as compared to the 30° branching. This is caused by the earlier onset of the branch curvature in the 60° model.

Beginning with location 'C75', the differences in SMIF are reduced, although the SMIF values for the bifurcation with the higher branching angle are elevated. This is caused by the higher level of kinetic energy 'stored' in the secondary motions in the central zone of the 60° branching bifurcation.

Regarding these simulations, the axial profiles are very similar for different branching angles, both for inspiration and expiration.

Experiments show very inconsistent results for the influence of the branching angle on secondary velocity (Chang and El Masry, 1982; Isabey and Chang, 1982). On the one hand, this is due to the complex inter-bifurcation effects occurring when coupling several branches, on the other hand due to experimental difficulties.

Marked differences, however, occur in the intensity of secondary motions. The SMIF values for a 30° branching for inspiration (using location 'D1r') and expiration (using location 'P0r') are 24.5% and 16.3%, respectively. For a 60° branching, these values are 31.3% and 22.8%. This corresponds to an increase of 28% for inspiration and an increase of 40% for expiration.

The influence of the branching angle is a minor one for axial profiles, but cannot be neglected for secondary velocities and thus for particle deposition calculations.

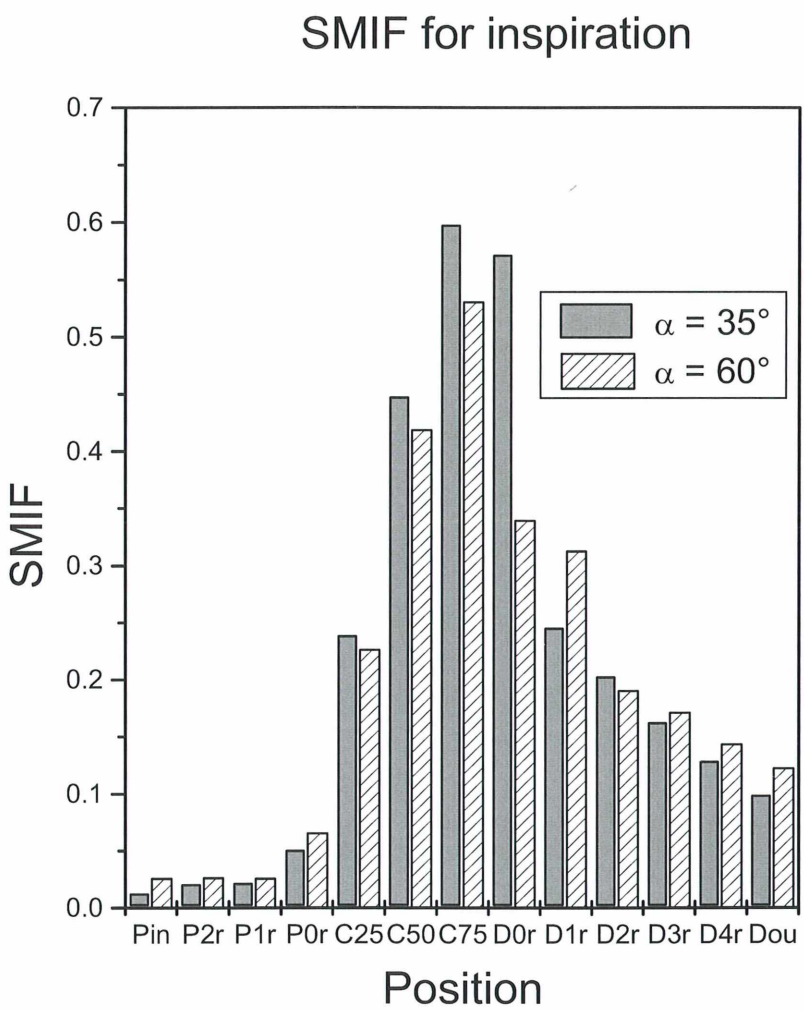

Figure 10
SMIF values for different positions for inspiration (flow rate is 120 l min^{-1}) and two branching angles (35° and 60°).

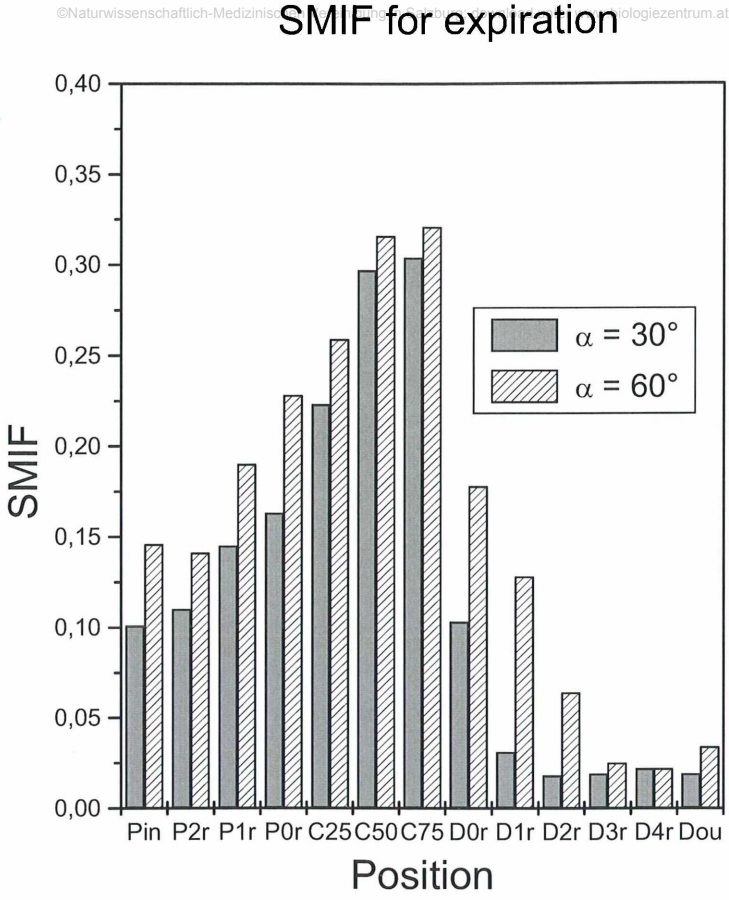

Figure 11 SMIF values for expiration (tracheal flow rate: 120 l min^{-1}) and different branching angles (35° and 60°).

Discussion

In this work some emphasis has been placed on the complicated secondary velocity components of the air flow in bifurcations, which amount up to 50% of the mean inlet velocity. Regarding the fate of particles in the size range of 0.5 µm, which practically follow the streamlines (Ultman, 1985), it can be imagined that the secondary flow is able to redistribute the particle density profile entering a bifurcation. At inspiration, particles could be transported to the vicinity of the carinal ridge, where they experience very strong outbound velocity components, thus initiating the typical twofold vortex pattern. This is a region of very high axial flow

contribution. With SMIF values of about 50%, these particles travel per time unit only twice as far downstream as in radial direction (provided that SMIF does not change dramatically). Particles therefore can be shifted from regions with very high axial velocities to regions with very low axial velocities. In general, the radial velocities are rather small here too. So not only the so-called 'jet effect' can contribute to bolus dispersion (Rosenthal et al., 1992; Rao et al., 1993; Briant and Lippmann, 1993; Schulz et al., 1995), but secondary motions may even play a more important role.

The flow in bifurcating tubes, especially in 'physiologically realistic bifurcation' models, is of rather complex nature. Unexpected behavior of flow occurs close to the carinal ridge, both for inhalation and exhalation. The 'secondary motion intensity factor' (SMIF) is introduced to describe overall features of the characteristics of radial flow. Large differences in the SMIF factor for different locations, for different geometries, and for different branching angles could be found.

In conclusion it can be stated that the PRB model in general exhibits more homogenous flow patterns with less pronounced gradients of primary and secondary flow components. However, the flow also shows reverse characteristics in the vicinity of the carinal ridge, which may have major impacts on particle deposition phenomena (Balásházy et al., 2003). When considering the parent branch, upstream influences of the flow dividing region must not be neglected for the development of primary and secondary flows. It could be demonstrated, that SMIF is a well-suited indicator for localized aerosol deposition.

Acknowledgements

This research was funded in part by CEC Contract No. FIGD-CT2000-00053.

References

ASGHARIAN, B., and ANJILVEL, S. Inertial and gravitational deposition of particles in a square cross section bifurcating airway. Aerosol Sci. Technol. 20: 177-193, 1994.

BALÁSHÁZY, I. Simulation of particle trajectories in bifurcating tubes. J. Comput. Phys. 110: 11-22, 1994.

BALÁSHÁZY, I, and HOFMANN, W Particle deposition in airway bifurcations I: Inspiratory flow. J. Aerosol Sci. 24: 745-772, 1993.

BALÁSHÁZY, I, and HOFMANN, W. Deposition of aerosols in asymmetric airway bifurcations. J. Aerosol. Sci. 26: 273-292, 1995.

BALÁSHÁZY, I, and HOFMANN, W. and MARTONEN, T.B. Inertial impaction and gravitational deposition of aerosols in curved tubes and bifurcations. Aerosol Sci. Technol. 13: 308-321, 1990.

BALÁSHÁZY, I., HEISTRACHER, T., and HOFMANN, W Air flow and particle deposition patterns in bronchial airway bifurcations: The effect of different CFD models and bifurcation geometries. J. Aerosol Med. 9: 287-301, 1996.

BALÁSHÁZY, I, and HOFMANN, W.and HEISTRACHER, T. Local particle deposition patterns may play a key role in the development of lung cancer. J. Appl. Physiol. 94: 1719-1725, 2003.

BRIANT, J.K., and LIPPMANN, M. Aerosol bolus transport through a hollow airway cast by steady flow in different gases. Aerosol Sci. Technol. 19: 27-39, 1993.

CHANG, H.K., and EL MASRY, O.A. A model study of flow dynamics in human central airways. Part I: Axial velocity profiles. Respir. Physiol. 49: 75-95, 1982.

FINLAY, W.H., STAPELTON, K.W., and YOKOTA, J. On the use of computational fluid dynamics for simulating flow and particle deposition in the human respiratory tract. J. Aerosol Med. 9: 329-341, 1996.

GRADON L., and ORLICKI D. Deposition of inhaled aerosol particles in a generation of the tracheobronchial tree. J. Aerosol Sci. 21: 3-19, 1990.

GUAN X., and MARTONEN, T.B. Flow transition in bends and applications to airways. J. Aerosol Sci. 31: 833-847, 2000.

HAMMERSLEY, J.R., and OLSON, D.E. Physical models of the smaller pulmonary airways. J. Appl. Physiol. 72: 2402-2414, 1992.

HEISTRACHER, T. Numerical simulation of airflow and particle deposition in bronchial airway bifurcation models. Ph.D. thesis at the University of Salzburg, Austria, 1996.

HEISTRACHER, T., and HOFMANN, W Simulation of airflow in a physiologically realistic airway bifurcation model. J. Aerosol Sci. 25, Suppl.1: S549-S550, 1994.

HEISTRACHER, T., and HOFMANN, W Physiologically realistic models of bronchial airway bifurcations. J. Aerosol. Sci. 26: 497-509, 1995.

HEISTRACHER, T., BALÁSHÁZY, I., and HOFMANN, W. The significance of secondary flows for localized particle deposition in bronchial airway bifurcations. J. Aerosol Sci. 26, Suppl. 1: S615-S616, 1995.

HOFMANN, W BALÁSHÁZY, I, and HEISTRACHER, T. The relationship between secondary flows and particle deposition patterns in airway bifurcations. Aerosol Sci. Technol. 35: 958-968, 2001.

HORSFIELD, K., DART, G., OLSON, D.E., FILLEY, G.F., and CUMMING, G. Models of the human bronchial tree. J. Appl. Physiol. 31: 207-217, 1971.

INTERNATIONAL COMMISSION ON ADIOLOGICAL PROTECTION (ICRP). Human Respiratory Tract Model for Radiological Protection. ICRP Publication 66, Annals of the ICRP, Vol. 24, Nos. 1-3, Elsevier, New York, 1994.

ISABEY, D., and CHANG, H.K. A model study of flow dynamics in human central airways. 2. Secondary flow velocities. Respir. Physiol. 49: 97-113, 1982.

KINSARA, A.A., TOMPSON, R.V., and LOYALKA, S.K. Computational flow and aerosol concentration profiles in lung bifurcations. Health Phys. 64: 13-22, 1993.

MARTONEN, T.B., YANG, Y., and XUE, Z.Q. Effects of carinal ridge shapes on lung airstreams. Aerosol Sci. Technol. 21: 119-136, 1994.

MARTONEN, T.B., ZHANG, Z., YANG, Y., and BOTTEI, G. Gas transport processes in human airways. Inhal. Toxicol. 7: 303-318, 1995.

OLDHAM, M.J., PHALEN, R.F., and HEISTRACHER, T. Computational fluid dynamic predictions and experimental results for particle deposition in an airway model. Aerosol Sci. Technol. 32: 61-71, 2000

PEDLEY, T.J., SCHROTER, R.C., and SUDLOW, M.F. Gas flow and mixing in the airways. Bioengineering aspects of the lung. J. B. West (ed), Marcel Dekker, New York, 1977.

RAO, N.P., NAVASCUES, J., and DE LA MORA.J. Aerodynamic focusing of particles in viscous jets. J. Aerosol Sci. 24: 879-892, 1993.

ROSENTHAL, F.S., BLANCHAR, J.D., and ANDERSON, P.A.I. Aerosol bolus dispersion and convective mixing in human and dog lungs and physical models. J. Appl. Physiol. 7: 862-873, 1992.

SCHROTER, R.C., and SUDLOW, M.F. Flow patterns in models of the human bronchial airways. Respir. Physiol. 7: 341-355, 1969.

SCHULZ, H., SCHULZ, A., BRAND, P., TUCH, T., VON MUTTIUS E., ERDL, R., REINHARDT, D., and HEYDER, J. Aerosol bolus dispersion and effective airway diameters in mildly asthmatic children. Eur. Respir. J. 8: 566-573, 1995.

TSUDA, A., SAVILONIS, B.J., KAMM, R.D., and FREDBERG, J.J. Periodic flow at airway bifurcations. III. Energy dissipation. J. Appl. Physiol. 69: 562-569, 1990.

ULTMAN, J.S. Gas transport in the conducting airways. In: Gas Mixing and Distribution in the Lung. L.A. Engel and M. Paiva (eds.), Marcel Dekker, New York, 1985.

WEIBEL, E.R. Morphometry of the Human Lung. Springer, Berlin, 1963.

YUNG, C.N., DE WITT, K.J., and KEITH, T.G. JR. Three-dimensional steady flow through a bifurcation. ASME J. Biomech. Eng. 112: 189-197, 1990.

ZHANG, Z., KLEINSTREUER, C., and KIM, C.S. Cyclic micron-size particle inhalation and deposition in a triple bifurcation lung airway model. J. Aerosol Sci. 33: 257-281, 2002.

ZHAO, Y., CITRINITI, J.H., and LIEBER, B.B. Flow characteristics in a symmetric bifurcation. ASME Adv. Bioeng. 22: 489-492, 1992.

ZHAO, Y., and LIEBER, B.B. Steady Inspiratory flow in a model symmetric bifurcation. ASME J. Biomech. Eng. 116: 488-496, 1994a.

ZHAO, Y., and LIEBER, B.B. Steady expiratory flow in a model symmetric bifurcation. ASME J. Biomech. Eng. 116: 318-323, 1994b.

Anschrift der Verfasser: [1] Institute of Physics and Biophysics
University of Salzburg
Hellbrunnerstraße 34
A-5020 Salzburg

[2] Polytechnic University of Salzburg
Department of
Informatics and Software Engineering
Schillerstraße 30
A-5020 Salzburg